

EFFECT OF REDUCING TEMPERATURE ON THE STRUCTURAL, ELECTRICAL AND MAGNETIC PROPERTIES OF POLY-CRYSTALLINE MATERIAL $\text{La}_{0.67}\text{Sr}_{0.20}\text{Cu}_{0.10}\square_{0.03}\text{MnO}_3$

H.W. ZHAO^{a*}, Y.L. LI^b, L.C. HU^c, C.R. CHANG^a, C.L. YAN^d

^aCollege of Science, North China University of Science and Technology, Tangshan 063009, Hebei Province, China

^bHebei Provincial Key Laboratory of Inorganic Nonmetallic Materials, North China University of Science and Technology, Tangshan 063009, Hebei Province, China

^cDepartment of Basic Teaching, Tangshan College, Tangshan 063000, Hebei Province, China

^dAnalysis & Testing Center, North China University of Science and Technology, Tangshan 063009, Hebei Province, China

$\text{La}_{0.67}\text{Sr}_{0.20}\text{Cu}_{0.10}\square_{0.03}\text{MnO}_3$ (“ \square ” representing cation vacancy) poly-crystalline manganite powder was synthesized by sol-gel method, which we used as parent materials. The parent powders were reduced by hydrogen in different temperature, and series of reduced powders were prepared. The bulk samples were sintered in Ar and air atmosphere respectively. Their structure, morphology, electrical and magnetic properties as well as magnetoresistance (MR) were researched in detail. Under an applied magnetic field of 1.8T, the maximum values of MR, MR_p , of the samples sintered in Ar atmosphere for 12 hours at 1100°C, with the power reduced for 15 minutes in different temperature (200°C, 250°C, 300°C) hydrogen atmosphere for $\text{La}_{0.67}\text{Sr}_{0.20}\text{Cu}_{0.10}\square_{0.03}\text{MnO}_3$ parent powders, respectively, were improved comparing to one of the sample sintered with the parent sample. The MR_p of the sample sintered with parent powder is 24.6% at 319K; the MR_p of the sample sintered with powder reduced for 15 minutes at 250°C, reaches 31.5%.

(Received January 14, 2016; Accepted March 7, 2016)

Keyword: Colossal magnetoresistance, Perovskite type structure, Sol-gel method, Reducing method

1. Introduction

Manganite $R_{1-x}T_x\text{MnO}_3$ with ABO_3 perovskite structure, where R and T are rare earth and alkaline earth ions, respectively, has been extensively studied due to its abundant physics related to colossal magnetoresistance (CMR) and its potential application in magnetic devices^[1-4]. In general, the MR magnitude of a perovskite manganite reaches the maximum only at the Curie temperature (T_C), which is beyond the room temperature region generally. And the MR changes abruptly with the temperature approaching the Curie temperature. These properties severely limit the practical applications of these materials^[5-8]. Many researches have thus been concentrated on making new material system that provides low field magnetoresistance (LFMR) around room temperature. On the other hand, recent efforts to broaden the CMR temperature range have been made by means of the Mn-site substitution or oxygen-deficiency^[9-12]. M.Brando^[9] et al studied the dependence of oxygen deficiency on electrical and magnetic properties of $\text{La}_{0.85}\text{Na}_{0.15}\text{MnO}_3 \cdot \delta$ ($\delta = 0; 0.04; 0.10$),

* Corresponding author: zhaoweihong2001@aliyun.com

they found that: when the δ increased, the Curie temperature of the samples decreased. X.M. Liu^[11] et al studied the electrical properties and magnetoresistance effect, found that: for $\text{La}_{0.67}\text{Sr}_{0.33}\text{MnO}_3$, Sr-site substituted by Cu and the leading in of vacancy could both change the peak temperature (T_{MR}) of *MR* to room temperature and improve the peak value of *MR*.

In this paper, we chose $\text{La}_{0.67}\text{Sr}_{0.20}\text{Cu}_{0.10}\square_{0.03}\text{MnO}_3$ as parent materials because its T_{MR} is higher than room temperature and its *MR* value a little bigger. By means of reducing the powders in different Temperature hydrogen atmosphere, changing the oxygen content of the parent materials, the peak value of *MR* are improved.

2. Experiment

Composite samples of $\text{La}_{0.67}\text{Sr}_{0.20}\text{Cu}_{0.10}\square_{0.03}\text{MnO}_3$ were prepared by the sol-gel method^[12], which we used as parent materials. This method has the advantage of using low-temperature synthesis, which not only results in smaller grains but also produces high-purity and homogeneous samples. Stoichiometric quantities of La_2O_3 , $\text{Sr}(\text{NO}_3)_2$, $\text{Cu}(\text{NO}_3)_2$ and $\text{Mn}(\text{NO}_3)_2$ were dissolved in dilute HNO_3 solution; suitable amounts of citric acid and ethylene glycol as complexing agent were added, until a completely homogeneous transparent solution was achieved. This solution was subjected to slow evaporation at 360K until a highly viscous residue was formed. Finally a gel was developed during heating at 473K for 24 h. The gel was thermally treated at 873K for 5 h for the purpose of organic precursor decomposition. After grinding, the samples were calcined in air at 1073K for 10 h until furnace cooling.

The parent powder samples were reduced by hydrogen in different conditions. First, put the parent powder samples in reducing furnace, and then inlet Ar gas for 10 minutes to outlet air in the furnace. Second, inlet the hydrogen and increase temperature for reducing need, then keep the temperature stable for the time we want. Third, after reducing process finished, the furnace cools in the hydrogen atmosphere until 50°C, then stops inletting hydrogen and inlet Ar to outlet the hydrogen in the furnace.

The $\text{La}_{0.67}\text{Sr}_{0.20}\text{Cu}_{0.10}\square_{0.03}\text{MnO}_3$ parent and reduced powders were pressed into pellets and then sintered in air at 1373K for 14 h followed by furnace cooling. Finally the bulk samples were gained.

The phase identification of samples has been performed using X-ray diffraction (XRD) with an 18kW Rigaku max-RB diffractometer with $\text{Cu K}\alpha$ radiation. The magnetization measurement was carried out with a Lake Shore vibrating sample magnetometer (VSM) in the temperature region of 300–380K. In order to determine the Curie temperature, we plotted a curve of $d\sigma/dT$ along the curve of special magnetization versus temperature. All the Curie temperature measurements were performed at a field of 0.05T. The morphologies of the powder samples were obtained using an S-570 Scanning Electron Microscopy (SEM). The temperature and magnetic field dependence of the resistivity were measured using Physical Property Measurement System (PPMS) with the standard dc four-probe method with the applied field vertical to the direction of the current.

3. Results and discussion

3.1 X-ray characterization

The structural characterization of the powder samples grinding from the bulk samples was determined. Fig.1 shows X-ray diffraction patterns for bulk samples B1-B4. Conditions of powder reducing and bulk sintering are given in table 1. The results indicate that our samples are composites composed of a $R\bar{3}c$ perovskite phase. The $\text{La}_{0.67}\text{Sr}_{0.20}\text{Cu}_{0.10}\square_{0.03}\text{MnO}_3$ parent sample B1 has a very few Mn_3O_4 phase indicated by XRD diffraction peaks $2\theta=36.12$ degree. As

the reducing temperature increasing for the powders, the Mn_3O_4 impurity phase in the samples could decrease or disappear. The sample B4 has already a purity phase of perovskite structure.

We use a Rietveld refinement software Fullprof suite to calculate the lattice parameter and crystal cell volume. The results are given in table 1. Compared with mother sample B1, the lattice constant, crystal cell volume of reduced samples B2-B4 has increased slightly, this may be because the oxygen vacancies make the lattice structure distortion

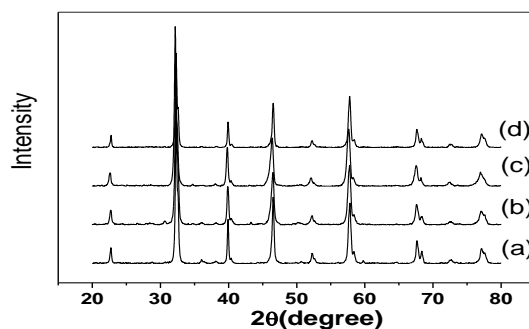


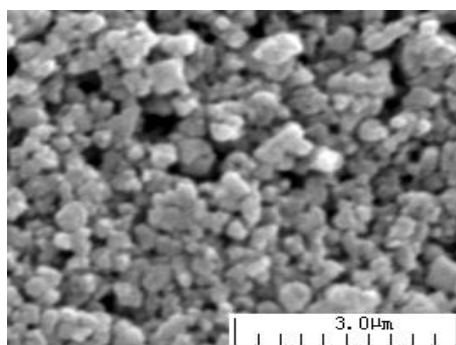
Fig.1 X-ray diffraction patterns for bulk samples B1(a), B2(b), B3(c) and B4(d)

Table.1 Conditions of powder reducing and bulk sintering and Lattice parameters, crystal cell volume for $La_{0.67}Sr_{0.20}Cu_{0.10}\square_{0.03}MnO_3$ bulk samples

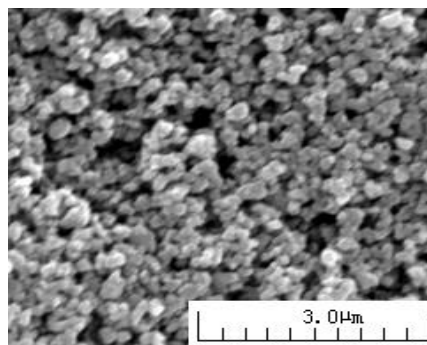
No.	Powder reducing condition		Bulk sintering condition		Lattice parameters		crystal cell volume $V(\text{\AA}^3)$
	$T_R(^{\circ}C)$	$t_R(\text{min})$	$T_S(^{\circ}C)$	$t_S(\text{hr})$	$a(\text{\AA})$	$c(\text{\AA})$	
B1	parent	parent	1100	12	5.5273	13.371	353.77
B2	200	15	1100	12	5.5325	13.376	354.58
B3	250	15	1100	12	5.5336	13.507	358.19
B4	300	15	1100	12	5.5316	13.375	354.43

3.2 Morphology of the powder sample

Fig.2 shows the scanning electron microscopy (SEM) morphology of powder samples B1, B3. From Fig.2 we can see that the $La_{0.67}Sr_{0.20}Cu_{0.10}\square_{0.03}MnO_3$ parent sample B1 prepared by sol-gel method possesses homogeneously globular shape grains, the grain size is about 100 nm. After being reduced by hydrogen, the phenomenon of conglomeration in particles was improved.



(a) Sample B1



(b) Sample B3

Fig.2 SEM morphology of powder samples B1 and B3

3.3 Magnetic properties of samples

Fig.3(a) shows curves of the special magnetization σ versus temperature T for the bulk samples, under an applied magnetic field of 0.05T. Fig.3(b) shows curves of the $d\sigma/dT$ calculated from Fig.3(a) versus temperature, in which the Curie temperatures (T_C) of the samples are determined by $d\sigma/dT$ tending to zero. Fig.4 shows the magnetic hysteresis loop of the bulk samples at room temperature (300K).

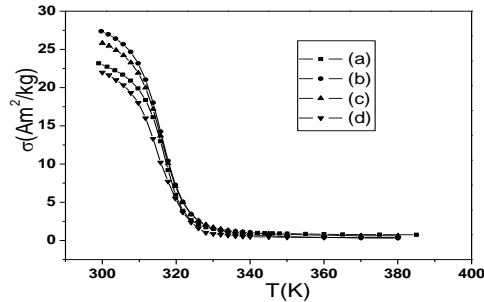


Fig. 3(a) Curves of special magnetization σ versus temperature for bulk samples B1(a), B2(b), B3(c) and B4(d), the applied magnetic field $\mu_0H = 50mT$

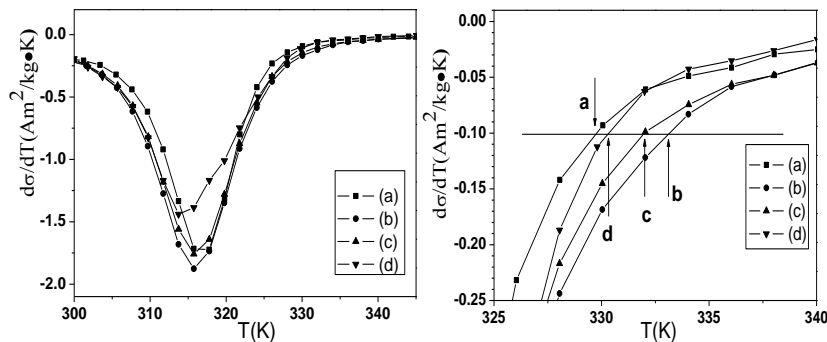


Fig.3(b) Curves of $d\sigma/dT$ calculated from Fig.3(a) versus temperature T for samples B1(a), B2(b), B3(c) and B4(d)

Fig 3(a) shows that in the temperature region measured, The samples experienced a ferromagnetic to the paramagnetic shift, the changes have gone through a transition region, due to Samples still in the transition zone show varying degrees of ferromagnetism, so we define $d\sigma/dT$ tend to zero corresponding to the temperature as the Curie temperature T_C . It can be seen from Figure 3(b) that the Curie temperature T_C of bulk samples B1 is about 329.7K. The Curie temperature of Bulk samples B2, B3 and B4 is 333.1K, 332.0 K and 330.3K respectively, as shown by Table 2. We can see that the Curie temperature of the samples is higher than room temperature, the samples at room temperature are ferromagnetic, reducing treatment changes Curie temperatures T_C of the sample not obvious.

Fig.4 shows that the magnetization basically reached saturation near 400mT.the samples are soft magnetic materials with small coercivity. Table.2 shows the special saturation magnetization σ (Am²/kg). It can be seen from Table.2 that: reducing temperature has a certain influence on special saturation magnetization σ , as the reducing temperature increased, the special saturation magnetization σ of samples first increases and then decreases, the sample B2 has the maximum σ ,reaching 45.8 Am²/kg.

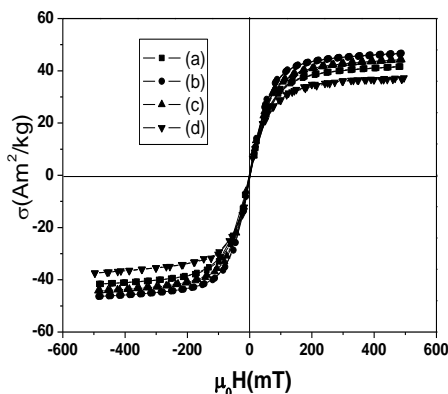


Fig. 4 The magnetic hysteresis loop of the samples B1(a), B2(b), B3(c) and B4(d) at 300K

Table.2 The Curie temperature T_C (K), special saturation magnetization σ (Am²/kg), metallic- semiconducting transition temperature T_{MI} (K), the maximum value MR_P (%) of the magnetoresistance, and the temperature T_{MR} (K) corresponding MR_P for $La_{0.67}Sr_{0.20}Cu_{0.10}\square_{0.03}MnO_3$ parent and reduced samples

No	T_R (°C)	T_C (K)	σ (Am ² /kg)	T_{MI} (K)	T_{MR} (K)	MR_P (%)
B1	parent	329.7	41.1	320	319	24.6
B2	200	333.1	45.8	333	318	27.6
B3	250	332.0	43.7	335	319	31.5
B4	300	330.3	36.7	332	318	25.9

3.4 Electrical and Colossal magnetoresistance properties of samples

The temperature dependence of the resistivity measured in zero field for the samples B1(a), B2(b), B3(c) and B4(d) are plotted in Fig.5. From Fig.5 we know that with the increase of temperature, the conductivity of the samples experienced a metal-semiconductor transition. Definition metal-semiconductor transition temperature T_{MI} for resistivity and temperature curve of resistivity maximum point corresponds to the temperature. The T_{MI} of reduced samples are higher than parent sample. The resistivity of the reduced samples was significantly lower than that of the parent sample, The reducing treatment makes the Mn_3O_4 impurity phase in the samples disappeared, which resulted in the decrease of the resistivity.

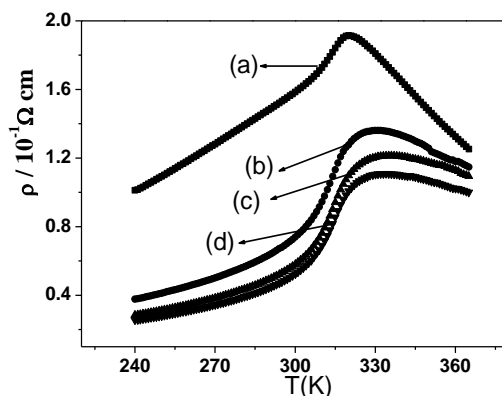


Fig. 5. Temperature dependence of the resistivity measured in zero field for bulk samples B1(a), B2(b), B3(c) and B4(d).

Temperature dependence of the resistivity measured in zero field and in an applied field (1.8T) for sample B3 are plotted in Fig.6. The corresponding magnetoresistances are also indicated.

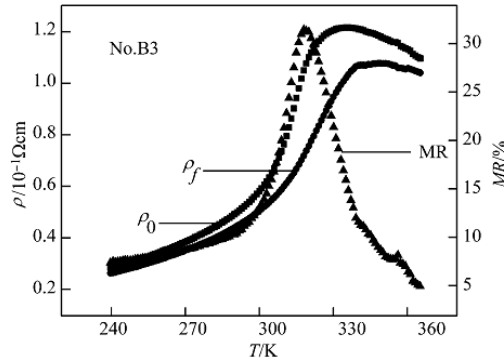


Fig. 6 Temperature dependence of the resistivity measured in zero field and in an applied field (1.8T) for sample B3. The corresponding magnetoresistances are also indicated.

From Fig.6 we know that in an applied magnetic field, the resistivity of the samples was significantly down. Define the magnetoresistance by $MR(\%) = [(\rho_0 - \rho_H) / \rho_0] \times 100\%$, where ρ_0 and ρ_H stand for the resistivities at 0 and 1.8 T.. The magnetoresistances of the sample B3 first increases and then decreases with the temperature increasing, and reaches its peak at the temperature $T_{MR} = 319K$, The Magnetoresistance peak value of the sample B3 reaches 31.5%.

Temperature dependence of magnetoresistance under an applied field of 1.8T for bulk samples B1(a)、B2(b)、B3(c) and B4(d) are plotted in Fig.7.

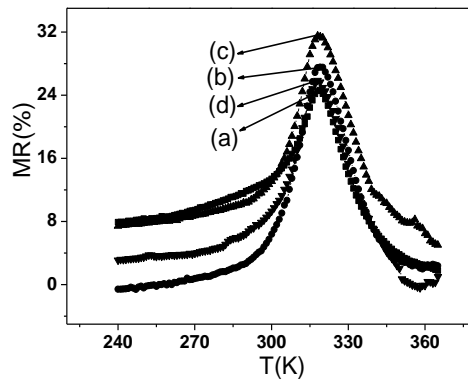


Fig. 7 Temperature dependence of magnetoresistance under an applied field of 1.8T for bulk samples B1(a)、B2(b)、B3(c) and B4(d)).

As shown in Figure.7, for parent samples B1, its $M_{RP} = 24.6\%$, and its $T_{MI} = 319K$. For the reduced samples B2(b)、B3(c) and B4(d), their T_{MI} changes very little, But their M_{RP} significantly increases, For the sample B3, which was reduced at the temperature $250^\circ C$, its M_{RP} improved the most significantly, reaches 31.5%. The magnetoresistance Peak value M_{RP} and the peak temperature T_{MR} of the samples are listed in Table.2

The Magnetoresistance effect is caused by the double exchange action between Mn^{3+} and Mn^{4+} ions^[13], The magnetoresistance peak value M_{RP} of reduced samples B2-B4 were obviously higher than that of mother sample B1. The reason is: reducing treatment makes the sample oxygen vacancies, Which resulted in the sample lattice structure distortion, and changes the bond length and bond Angle of $\text{Mn}^{3+}-\text{O}^{2-}-\text{Mn}^{4+}$ ions, Meanwhile changes the ratio between Mn^{3+} and Mn^{4+} , strengthen the double exchange action and then makes the peak value of magnetoresistance larger.

Applied field dependence of the magnetoresistance measured at 300K for sample B3 is plotted in Fig.8. Fig.8 shows that: when the magnetic field increased, the magnetoresistance increases monotonously. With the magnetic field achieving 6T, the magnetoresistance reaches 35% and has not yet reached saturation.

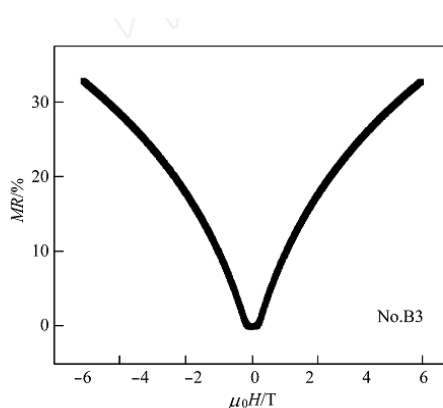


Fig. 8 Applied field dependence of the magnetoresistance measured at 300K for sample B3

4. Conclusions

We studied the effect of reducing temperature on the structural, electrical and magnetic properties of poly-crystalline material $\text{La}_{0.67}\text{Sr}_{0.20}\text{Cu}_{0.10}\square_{0.03}\text{MnO}_3$. The reducing time was 15 minutes, the reducing temperature was 200°C, 250°C and 300°C respectively. It was found that: the reducing process did not change the samples of the perovskite structure, but with the increase of the reducing temperature, the Mn_3O_4 impurity phase with the properties of insulator in the samples decreased gradually, and then disappeared, which resulted in the decrease of the resistivity. The reducing temperature had no obvious effect on the peak temperature of the magnetoresistance.

Appropriate reducing temperature can make the peak value of the magnetoresistance M_{RP} significantly increased, but too much high reducing temperature also can lead to M_{RP} decreased.

Compared with mother sample B1, the sample B3, which was reduced at the temperature 250°C, its M_{RP} improved the most significantly, increased from 24.6% (B1) to 31.5% (B3).

Acknowledgements

This work was supported by Science and Technology Support Project of Hebei Province, China (Grant No. 15211111); Science and Technology Research Program for Colleges and Universities in Hebei Province, China (Grant No. Z2012002); Science and Technology Research Program for Colleges and Universities in Hebei Province, China (Grant no. Z2014017).

References

- [1] Y.Tokura, T.Tomioka, *J. Magn. Magn. Mater.* **200**, 1 (1999) .
- [2] J.Fontcuberta, L.Balcells, M.Bibes, J.Navarro, C.Frontera, J.Santiso, J.Fraxedas, B.Martinez, S.Nadolski, M.Wojcik, E.Jedryka, M.J.Casanove, *J. Magn. Magn. Mater.* **242**, 98 (2002).
- [3] Chun-Hua Yan, Zhi-Gang Xu, Tao Zhu, Zhe-Ming, Fu-Xiang Cheng, Yun-Hui Huang, Chun-Sheng Liao, *J. Appl. Phys.* **87**, 5588 (2000) .
- [4] P.Chen, Y.W.Du, D.Y.Xing, *Phys. Rev. B* **64**, 4402 (2001).
- [5] L .Balcells, B.Martinez, F.Sandiumenge and J.Fontcuberta J, *J. Magn. Magn. Mater.* **211**, 193 (2000).
- [6] G.Q.Gong, G..Xiao, J.Z.Sun, A.Gupta, W.J.Gallagher, C.L.Canedy, *J. Appl. Phys.* **79**, 4538 (1996).
- [7] G.Xiao, G..Q.Gong, A.Gupta, C.L.Canedy, J,Z.Sun, E.J.Mcniff, *Phys. Rev. B* **54**, 6073 (1996).
- [8] R. Shreekala; M. Rajeswari; K. Ghosh, *Appl .Phys. Lett.* **71**, 282 (1997).
- [9] M. Brando, R. Caciuffo, J. Hemberger, et.al, *J. Magn. Magn. Mater.* **417** , 272 (2004)
- [10] N. Abdelmoula, K. Guidara, A. Cheikh-Rouhou, et al, *Journal of Solid State Chemistry* **151**, 139 (2000)
- [11] X. M. Liu, G. D.Tang, et.al, *J. Magn. Magn. Mater.* **277**, 118 (2004)
- [12] R. Shiozaki, K. takenake, and S. Sugai, *Phys. Rev. B.* **63**, 184419 (2001)
- [13] C Zener , *Phys Rev* ,**81**(3):440 (1951).